BIOCHEMISTRY
including biophysical chemistry & molecular biology
Article

Biochemistry **2011,** *50,* 37–47 37
DOI: 10.1021/bi101582p

The Synucleins Are a Family of Redox-Active Copper Binding Proteins

Paul Davies,[‡] Xiaoyan Wang,[‡] Claire J. Sarell,[∥] Alex Drewett,[‡] Frank Marken,[§] John H. Viles,[∥] and David R. Brown*[,‡]

[‡]*Department of Biology and Biochemistry, and* [§]*Department of Chemistry, University of Bath, Claverton Down, Bath BA27AY, U.K., and* [∥]*School of Biological and Chemical Sciences, Queen Mary, University of London, Mile End Road, London E14NS, U.K.*

Received September 30, 2010; Revised Manuscript Received November 29, 2010

ABSTRACT: Thermodynamic studies in conjunction with EPR confirm that α-synuclein, *β*-synuclein, and *γ*-synuclein bind copper(II) in a high affinity 1:1 stoichiometry. *γ*-Synuclein demonstrates the highest affinity, in the picomolar range, while α-synuclein and *β*-synuclein both bind copper(II) with nanomolar affinity. The copper center on all three proteins demonstrates reversible or partly reversible redox cycling. Various mutations show that the primary coordinating ligand for copper(II) is located within the N-terminal regions between residues 2−9. There is also a contribution from the C-terminus in conjunction with the histidine at position 50 in α-synuclein and position 65 in *β*-synuclein, although these regions appear to have little effect on overall coordination stability. These histidines and the C-terminus, however, appear to be critical to the redox engine of the proteins.

The 140-residue presynaptic protein α-synuclein (α-syn)[1] has been implicated in the pathogenesis of several neurodegenerative diseases that have now been termed the synucleinopathies. These disorders include Parkinson's disease (PD), Lewy body variant Alzheimer's disease, and dementia with Lewy bodies (DLB) (*1*). The pathology of these diseases is characterized by progressive neuronal loss and the presence of intracellular deposition of protein, predominantly α-syn, known as Lewy bodies (LBs). The location of these LBs is dependent on the disease. The LBs are found mainly within the substantia nigra in PD, the neocortex and brain stem in DLB, and amygdale in around 60% of Alzheimer's disease (AD) patients (*2*). α-syn is also the nonamyloid-*β* component of AD-associated amyloid (*3*). New evidence has also linked α-syn with multiple sclerosis (*4*).

There is strong evidence of links between mutations in the gene encoding α-syn and increased susceptibility to disease. The point mutations A30P, A53T, and E46K have been found in familial cases of PD (*5*−*7*). Additionally, genomic multiplications involving the α-syn gene are found in many families affected by dementia, PD, and DLB (*8*−*10*). Transgenic mice overexpressing α-syn have increased Lewy body formation, dopaminergic loss, and motor deficits (*11*). Downregulation of α-syn in the substantia nigra of rats rescues dopaminergic cells from death (*12*). This strongly suggests not only that α-syn is key to disease pathogenesis but also that the levels of the protein determine disease severity and speed of progression.

Despite the strong evidence for the involvement of α-syn in dementia, the mechanism by which it causes cell death is unknown. Additionally, the physiological function of the protein remains elusive. The protein has been shown to be highly expressed in certain regions of the brain (*13*). It has also been shown that, while largely unstructured in the cytoplasm, the protein adopts a more ordered and highly helical structure when associated with lipid membranes (*14*, *15*). Perhaps a key element in the elucidation of both the function and disease roles of α-syn is the discovery of the protein's ability to associate with metals, especially copper. The disruption of metal homeostasis in the brain is now strongly linked with the progression of neurodegeneration (*16*). High levels of copper, zinc, and iron are found in and around amyloid plaques in AD brains (*17*). High levels of copper are also found in the cerebrospinal fluid of PD brains(*18*). In addition, individuals with chronic industrial exposure to copper and iron−copper have an increased rate of PD (*19*). Also of great interest is the propensity of copper(II) to induce α-syn aggregation to a toxic oligomeric form (*20*).

There is very little consensus in the literature concerning the copper binding properties of α-syn. Initial analysis showed that α-syn is able to bind 5−10 copper ions with a K_d of 45−60 μM (*21*). However, a more recent analysis showed that α-syn binds to two copper(II) ions per monomer with a dissociation constant in the range of 0.1−50 μM and is able to bind more copper ions with much weaker affinity (*22*). α-syn has also been shown to bind iron(II) (*23*), with an affinity in the 1 mM range (*24*), and other cations including manganese(II), cobalt(II), nickel(II) (*24*), magnesium, and calcium (*25*, *26*). There has also been some controversy in the identification of the copper binding sites. Initial studies suggested that the C-terminus of α-syn was responsible for copper(II) binding (*21*, *27*). However, recent analysis of copper(II) binding to α-syn truncation mutants suggests this region is involved only in low-affinity binding, with the C-terminal carboxylate residues (119−123) likely to be the major contributors (*22*). A high-affinity Cu(II) binding site has been reported in the N-terminus, involving residues 3−9 and 49−52, which coordinate into a single Cu(II) binding interface (*22*). However, mutation of the identified coordinating ligand at histidine 50 to alanine appears to have no effect on copper(II) binding (*28*). Another study of metal binding to the N-terminal region of α-syn utilized peptides to show that Cu(II) ions appear to be coordinated by the N-terminal amine group of methionine (residue 1), the amide nitrogen, and the *β*-carboxylic group of

*Corresponding author. Phone: +44-1225-383133. Fax: +44-1225-386779. E-mail: bssdrb@bath.ac.uk.

[1]Abbreviations: α-syn, α-synuclein; CV, cyclic voltammatry; *β*-syn, *β*-synuclein; EPR, electron paramagnetic resonance spectroscopy; *γ*-syn, *γ*-synuclein; DLB, dementia with Lewy bodies; ITC, isothermal titration calorimetry; PD, Parkinson's disease.

Published on Web 11/30/2010

aspartic acid, residue 2 (*29*). Considering the potential links between α-syn, metals, and disease, there is a clear need for a detailed and rigorous assessment of copper(II) associations with the protein.

In addition to α-syn, the synuclein family also consists of *β*-synuclein (*β*-syn) and *γ*-synuclein (*γ*-syn). α-syn and *β*-syn are predominantly expressed in the brain with *β*-syn making up around 75−80% of the total brain synuclein content (*30*). *γ*-syn is found primarily in the peripheral nervous system (*31*). The three proteins are highly homologous, and there is evidence of mutation in the *β*-syn gene in cases of DLB (*32*). It is therefore of interest to assess the metal binding to these homologues.

The aims of this study were therefore to thoroughly assess the binding parameters of copper(II) to the synucleins. Electron paramagnetic resonance (EPR) imaging was used to assess the coordination environment for the metals while isothermal titration calorimetry was used to obtain accurate affinity and stoichiometry data. Cyclic voltammetry was then used to assess any redox properties of the metal centers when bound.

EXPERIMENTAL PROCEDURES

Purification of Synuclein Proteins. The genes for α-syn, *β*-syn, and *γ*-syn were amplified from human neuroblastoma cells and cloned into pET-3a expression vectors. Following transformation into BL21 *Escherichia coli* cells, untagged synuclein protein expression was induced at OD_{600} 0.5−1.0 with 1 mM IPTG for 4 h. Cells were harvested by centrifugation (8000*g*) and lysed enzymatically in 150 mM Tris-HCl, pH 8.0 (buffer A), 1 mM PMSF, and 50 *μ*g/mL DNase. After centrifugation at 10000*g*, the pellet was discarded, and the supernatant was loaded onto a 50 mL Q-Sepharose column (Amersham Biosciences). The column was washed with 100 mL of buffer A and then 2 column volumes of buffer A + 100 mM NaCl. Synuclein proteins were eluted with a broad gradient elution of 100 mM to 1 M NaCl (all synuclein proteins eluting at approximately 350 mM NaCl). SDS−PAGE analysis of Q-Sepharose fractions was performed, and fractions enriched for synuclein were pooled. Synuclein proteins were collected as flow-through from a PM30 cellulose membrane (Millpore) to remove any large molecular weight contaminants and then concentrated with a PM10 PES membrane (Millipore). Purified synuclein proteins were dialyzed extensively at 4 °C in Chelex-treated Milli-Q. Protein concentration was measured by absorbance at 275 nm with extinction coefficient 5600 M^{-1} cm^{-1} for α-syn and *β*-syn and 1400 M^{-1} cm^{-1} for *γ*-syn.

Mutagenesis. Constructs expressing α-syn, *β*-syn, and *γ*-syn were prepared as previously described above. Site-directed mutagenesis was then used to replace the codon of interest. Overlapping splint oligonucleotides were used for each site. Each round of mutagenesis was confirmed by DNA sequencing.

Oligonucleotide sequences (forward primers only): α-syn H50A, GAGGGAGTGGTGGCTGGTGTGGCAACAG; *β*-syn H65A, CAAGGAACAGGCCTCAGCTCTGGGAGGAGCTGTG; α-syn Δ2−9, GAAGGAGATATACATATGAAGGCCAAGGAGGGAGTTG; *β*-syn Δ2−9, AGGAGATATACATATGATGGCCAAGGAGGGCGTTGTGG; α-syn Δ119−126, CTGGAAGATATGCCTGTGATGCCTTCTGAGGAAGGG.

Isothermal Titration Calorimetry Measurements. ITC experiments were carried out on a Microcal VP-ITC. A series of injections of metal were made into an isolated chamber containing the protein at a constant temperature of 25 °C. Heat changes within the cell were monitored during each injection of metal and recorded as the total heat change per second over time. A binding isotherm was then fitted to data and expressed as heat change per mole of metal against the metal to protein ratio. From these data, a model is used to predict the number of binding sites on the protein involved in the reaction, the association constants of the binding (K_a), and the change in enthalpies (ΔH). Protein samples were prepared by adding a small amount of concentrated and pH-adjusted MOPS buffer to a final concentration of 100 mM buffer and either 50 or 100 *μ*M protein. Different concentrations were used to ensure that results were repeatable over a variety of conditions. The choice of buffers was based on initial trials, which revealed that these buffers offered the minimum of background noise. The use of free copper in the titrations results in protein aggregation and nonspecific binding (*33*). In addition, no free copper exists *in vivo* so a copper chelate was used. Copper solutions were prepared by adding copper sulfate to 100 mM buffer (as above) along with glycine in a molar ratio of 1:4. Glycine chelates copper, forming a $Cu(Gly)_2$ complex. The excess glycine thus ensures that there is never any free copper in the reaction cell, avoiding the complications mentioned above. Buffer was added to the metal to ensure that the strong acidity of copper sulfate did not overwhelm the buffering capacity of the protein solution. Titrations of copper sulfate (30 × 4 *μ*L) into an unbuffered protein solution show a total change of −1 pH (data not shown). The use of buffer in only one of the solutions would result in significant background noise so therefore both protein and metal solutions were buffered. The concentration of copper used was dependent on the concentration of protein in the reaction cell. The final ratio of protein to copper in the reaction cell after each ITC experiment was 1:5.

During each experiment, 30 × 4 *μ*L doses of copper were injected into the chamber of protein, which was stirred constantly at 300 rpm. Each injection was followed by a 2 min period to ensure equilibration of the solution. All experiments were repeated three times and where possible using different concentrations of separately prepared protein. Data were analyzed using models based on refs *34* and *35* using the Igor Pro software. Each experimental condition had a blank run with protein in the chamber replaced with buffer. These data were then subtracted from the run with protein present to take into account any energy of dilution or metal/buffer reaction. A binding isotherm was then fitted to the data using a least-squares calculation to obtain a χ^2 value. The isotherm that fitted with the lowest χ^2 was taken as the best fit model. From this model, values for K_a and ΔH were calculated along with the most likely number of binding sites involved. The K_a values were then adjusted to factor in the affinity of copper for glycine. Previous studies have shown glycine to bind two atoms of copper with affinities of $K_1 = 4.0 \times 10^5$ M^{-1} and $K_2 = 1.7 \times 10^4$ M^{-1} with $\beta_2 = 6.8 \times 10^9$ M^{-1} at pH 7 (*36*, *37*). These values also vary with pH. The relative contribution of each of these species at the prevalent pH was then used in the final equilibrium to fully account for the effect of the chelate, as previously reported(*38*). In addition, sequential modeling was carried out on data obtained from constructs at pH 7 and 8. For these models, final values were adjusted as previously shown (*37*).

Cyclic Voltammetry. The method to analyze synuclein electrochemistry is based on previous studies with the prion protein (*36*, *37*). Voltammetric measurements were conducted with a *μ*-Autolab III potentiostat system (Eco Chemie, The Netherlands) in a conventional three-electrode electrochemical

cell. Experiments were performed in staircase voltammetry mode (step potential 0.6 mV) with a platinum gauze counter and saturated calomel reference electrode (SCE, REF401; Radiometer). The working electrode used was a 3 mm diameter boron-doped diamond (Diafilm; Windsor Scientific, U.K.). Electrodes were polished on fresh microcloths (Buehler, U.K.) with alumina (1 μm; Buehler, U.K.) as polishing aid. After the final polish on a clean microcloth, electrodes were rinsed with demineralized water. Aqueous solutions were thoroughly deaerated with argon (BOC, U.K.) prior to recording data. All measurements were undertaken at 22 ± 2 °C.

Voltammetric measurements were conducted in aqueous buffer solution (20 mM MOPS, pH 7) thoroughly deaerated with argon. The working electrode was polished and the background current recorded in the absence of protein. Proteins were exposed to $CuSO_4$ at a 4:1 molar ratio to ensure saturation of the protein. Next, the working electrode was immersed into the protein solution (containing 100 μM recombinant synuclein in buffer) and after 60 s removed and rinsed with water to remove unbound protein and free copper. A longer incubation did not significantly increase the amount of immobilized protein. The resulting protein-modified electrode was reimmersed into the pure buffer solution in the measurement cell, and cyclic voltammograms were recorded always starting at open circuit potential. Protein adhesion to the boron-doped diamond electrode surfaces was excellent, and stable signals were obtained for many potential cycles.

Electron Paramagnetic Resonance Spectroscopy (*EPR*). Synuclein protein samples were prepared at a concentration of 100 μM in 20 mM *N*-ethylmorpholine (EM) buffer, pH 7. Different equivalents of Cu(II) were added into protein samples before they were transferred into the 3 mm internal diameter quartz EPR tubes and frozen in liquid nitrogen. The experiments were performed in a Bruker continuous-wave EPR spectrometer at a temperature of 20 K. The EPR spectrometer was operated at X-band microwave frequencies. All of the spectra were operated with 100 kHz magnetic field modulation, with modulation amplitude of 0.5 mT and microwave power of 2 mW. The data were analyzed and plotted in Peisach−Blumberg plots to assign coordinating ligands and geometry of metal binding sites of synuclein proteins.

RESULTS

Affinity and Stoichiometry of Copper(*II*) *to* α-*syn,* β-*syn, and* γ-*syn*. Isothermal titration calorimetry was used to accurately quantify the affinity and stoichiometry of copper(II) to the synucleins. In order to overcome the issues surrounding the solubility of copper at physiological pH, the metal was delivered as a chelate, in this case as a bis complex with glycine. We have previously shown that isothermal titration calorimetry can be successfully used to accurately quantify the affinity and stoichiometry of chelated copper(II) to complex macromolecules using a modified set of equations based on the fractional sequential binding models by Microcal (*37*). On analysis of the isotherms produced from the associations of copper(II) to the synucleins, it was clear that this sequential model was inappropriate for determination of binding parameters for these proteins. Others have successfully designed new equations to describe the binding of chelated metals to macromolecules (*34*, *35*), again based on the equations from Microcal. These models describe the binding of a chelated molecule to either one set (*34*) or two sets (*35*) of unrelated sites. These models were therefore used to analyze the thermodynamic data from these experiments. Figure 1 shows a representative ITC trace for the titration of chelated copper(II) into α-syn at pH 7.

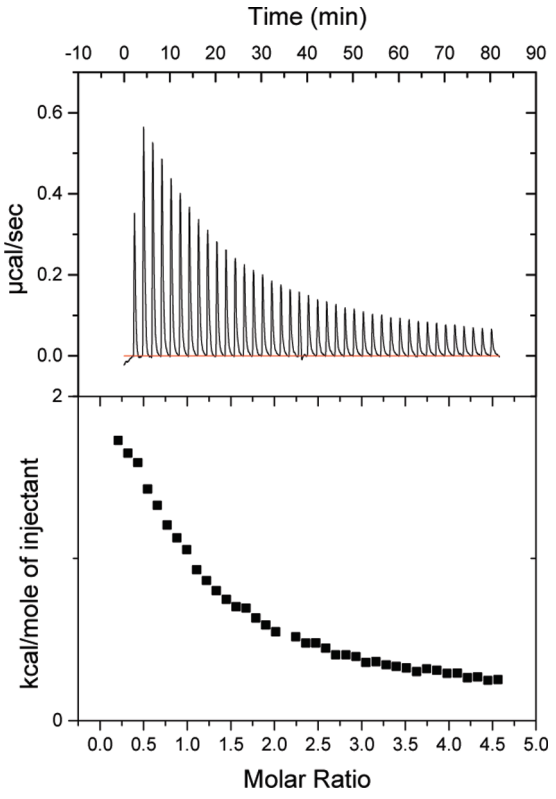

FIGURE 1: Typical ITC trace showing the titration of 5 mM copper-(II) sulfate chelated with 20 mM glycine into 100 μM wild-type recombinant α-syn in 100 mM MOPS buffer, pH 7 at 25 °C.

For α-syn, β-syn, and γ-syn the reaction was net endothermic due to the use of buffers. The total enthalpy change evident in the reaction is a sum of the reactions involving the disassociation of copper from glycine and its association with the proteins as well as the protonation changes involving the proteins, the chelator, and the buffer used. However, as each experiment was carried out using the same conditions, a direct comparison between experiments can be made in order to assign individual binding events to the log stability constants listed. Fitting of the isotherms to modified equations for either one set or two sets of sites produced the binding parameters described in Table 1.

The wild-type synucleins all bound a single molecule of copper(II) in one of two thermodynamically distinct modes. A dominant species, accounting for approximately 80% of analyzed proteins, demonstrated the highest affinity for copper(II). The protein exhibiting the highest affinity for copper(II) was γ-syn with a calculated disassociation constant in the dominant species of ~5 pM. The second species was also of high affinity, with a disassociation constant of ~29 pM. α-syn demonstrated high affinity binding in its dominant species with a disassociation constant of ~0.4 nM with the second species at ~63 nM. The weakest association with copper(II) was evident in β-syn, with the two species demonstrating disassociation constants of ~1 nM and ~2 μM.

In order to identify the key residues necessary for copper(II) coordination, multiple mutants were created, expressed, and purified with one or more putative copper binding regions replaced or removed. This analysis was carried out in both α-syn and β-syn. Previous reports have suggested the histidine at position 50 in α-syn

Table 1: Affinity and Stoichiometry of Copper(II) Binding to the Synucleins As Determined by ITC[a]

	n_1	log K_1 (M^{-1})	log ΔH ($\times 10^3$ kcal mol^{-1})	n_2	log K_2 (M^{-1})	log ΔH ($\times 10^3$ kcal mol^{-1})
α-syn	0.82 ± 0.09	9.43 ± 4.40	1.40 ± 0.1	0.25 ± 0.05	7.20 ± 2.78	10.66 ± 0.9
β-syn	0.72 ± 0.03	8.72 ± 4.02	1.54 ± 0.15	0.30 ± 0.02	5.77 ± 2.47	21.26 ± 1.07
γ-syn	0.80 ± 0.11	11.30 ± 6.90	2.24 ± 0.18	0.24 ± 0.01	10.53 ± 4.41	13.87 ± 0.31
α-syn Δ2−9	0.52 ± 0.04	7.28 ± 3.42	9.51 ± 1.71	0.50 ± 0.03	6.78 ± 2.46	5.38 ± 0.38
α-syn H50A	0.77 ± 0.03	10.13 ± 4.15	1.96 ± 0.03	0.26 ± 0.01	7.99 ± 0.68	10.90 ± 2.83
α-syn Δ2−9 H50A	0.72 ± 0.15	6.96 ± 2.52	33.11 ± 1.06	0.35 ± 0.03	6.91 ± 3.60	36.31 ± 1.64
α-syn10−100	0.66 ± 0.01	6.26 ± 1.29	8.56 ± 0.26	0.28 ± 0.02	6.00 ± 1.16	7.42 ± 0.72
α-syn10−100 H50A	0.88 ± 0.07	7.66 ± 3.14	9.55 ± 0.06	n/d	n/d	n/d
β-syn Δ2−9	1.04 ± 0.16	7.33 ± 3.36	8.05 ± 0.79	n/d	n/d	n/d
β-syn H65A	0.72 ± 0.07	9.04 ± 4.44	1.12 ± 0.14	0.29 ± 0.02	6.94 ± 2.44	17.50 ± 0.58
β-syn Δ2−9 H65A	0.56 ± 0.07	6.34 ± 2.02	21.10 ± 3.10	n/d	n/d	n/d
β-syn10−100 H65A	n/d	n/d	n/d	n/d	n/d	n/d

[a] n/d = not detected. In each case, the fit producing the lowest χ^2 value was used from either one or two sets of independent sites. The values represent the mean ± standard error from at least three independent experiments. n_1 = first binding site, n_2 = second binding site. K = affinity value, and ΔH = change in enthalpy.

and position 65 in β-syn, along with residues in the N-terminus, to be responsible for metal coordination. There have also been suggestions of contributions from the C-terminal region. To test this hypothesis, these regions were focused on for this study. Table 1 lists the binding data as determined by ITC for these mutants. For α-syn, replacing the histidine at residue 50 with alanine had no deleterious effect on copper coordination but indeed enhanced the stability of binding. The two species also demonstrated similar enthalpies of binding to those on the wild type, suggesting the removal of H50 had no significant effect. Removal of the first nine amino acids within the N-terminus, however, had a strikingly deleterious effect on binding stability and was further evidenced by a significant change in the enthalpies of binding. Interestingly, removal of the C-terminus did not appear to have a significant effect on binding, unless the histidine at residue 50 was also absent, suggesting that this histidine did contribute to the coordination of copper when the C-terminus was absent. In fact, only a single species was evident when H50 and the N- and C-termini were absent. Coordination of copper in the absence of these regions does suggest a further coordinating ligand that has yet to be identified. β-syn demonstrated a similar pattern of binding with the histidine at position 65 seeming to have a repressive effect on stability when present. Here again, it appears that residues 2−9 are the primary coordinating ligand for copper(II). β-syn, however, showed no copper(II) affinity when the N- and C-termini were removed.

Further confirmation of the observations from the ITC was achieved through electron paramagnetic resonance studies (EPR). Figure 2 shows the continuous-wave EPR spectra for copper(II) titration with the synucleins. All three proteins appeared to form similar copper(II) complexes. The EPR spectra indicate square-planar or tetragonal coordination geometry. Two sets of axial signals are observed which correspond to two binding modes for each protein, referred to as mode 1 and mode 2. The two modes were present at all copper(II) concentrations, at the same ratio throughout the titration, with mode 1 always the predominant one. Quantification of copper(II) binding by double integration of the EPR spectra revealed that the proportions of copper(II) bound by mode 1 and mode 2 in α-syn were 75% and 25%, respectively, in very good agreement with the thermodynamic data. The EPR spectra of both modes were typical of type II copper(II) centers with N and O ligands in a square-planar or tetragonal environment (*39*). The coordinating ligands were determined by the $A_{\|}$ and $g_{\|}$ parameters, which were plotted using Peisach−Blumberg diagrams, suggesting 2N2O (mode 1) and 3N1O (mode 2) coordination spheres for all three proteins (Table 2). We note that the two binding modes do not load copper(II) ions sequentially but retain the same relative proportions throughout the Cu(II) titration. This titration behavior suggests that the two binding modes are interrelated and share three of the same ligands while the fourth is interchangeable between a nitrogen and oxygen ligand.

Redox Properties of the Copper-Bound Synucleins. We have previously shown interesting redox properties for proteins with stable copper(II) binding properties (*36*, *37*). In order to investigate these properties in the synucleins, linear sweep cyclic voltammetry was employed to fully explore the electron transfer capabilities of the proteins. Our previous work demonstrated that it was possible to immobilize proteins on boron-doped diamond electrodes based on their electrostatic properties(*37*). These surfaces carry a negative charge. A charge distribution analysis of α-syn (Figure 3a) revealed a highly polar distribution with a strong positive charge within the N-terminus and strong negative charge within the C-terminus, allowing electrostatic adsorbance to the electrode via the N-terminal region. Similar distributions were evident for β-syn and γ-syn (data not shown). Figure 3b shows the voltammetric trace for copper(II)-loaded α-syn at increasing scan rates from 10 to 80 mV s^{-1}.

For each scan rate, two clear peaks are evident, a positive peak corresponding to an oxidation phase and a more negative peak corresponding to a reduction phase. In each case, the experiment was started from a open circuit potential. Continuous cycling of the potential produced no detectable change in peak intensity. As the scan rate increased, peak potential and peak current altered in a predicted fashion. Figure 3c shows a logarithmic relationship between peak potential and scan rate, and Figure 3d shows a linear relationship between peak current and scan rate. This confirmed a permanently surface bound protein and electron transfer directly into the protein-bound copper (*37*). This indicates that the absorption of the protein was stable and the current responses were highly reproducible and reversible. The characteristic logarithmic dependence was consistent with an electron transfer rate-limited process, which was represented by the equation (*37*)

$$E_p = E_{mid} + \frac{RT}{\alpha F} \ln\left(\frac{RTk^0}{\alpha F v}\right)$$

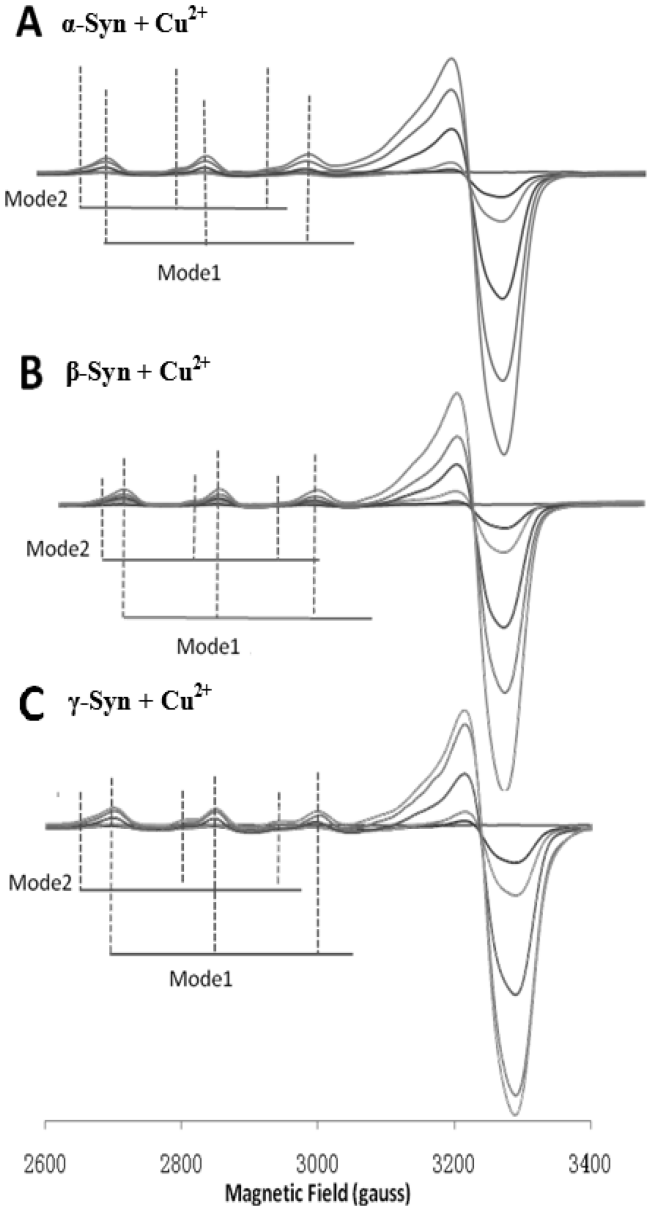

FIGURE 2: Continuous-wave EPR of copper(II) binding to wild-type (A) α-syn, (B) β-syn, and (C) γ-syn bound to 1, 2, 3, and 4 mol equiv of copper(II) at pH 7. Two copper(II) binding modes were indicated for all three proteins. Synuclein protein samples were prepared at a concentration of 100 μM in 20 mM *N*-ethylmorpholine (EM) buffer.

Table 2: Comparison of Spin Hamiltonian Parameters of Copper(II) Binding Modes for α-syn, β-syn, γ-syn at pH 7.4

		$A_{\|\|}$(mK)	$g_{\|\|}$	coordination
α-syn	mode 1	14.0	2.29	2N2O
	mode 2	13.0	2.33	3N1O
β-syn	mode 1	13.9	2.29	2N2O
	mode 2	12.9	2.33	3N1O
γ-syn	mode 1	14.1	2.29	2N2O
	mode 2	13.2	2.33	3N1O

In this equation the peak potential E_p is correlated to the midpoint potential, E_{mid}, the gas constant, R, the absolute temperature, T, the transfer coefficient, α, the Faraday constant, F, the standard rate constant for electron transfer, k^0, and the scan rate, v.

It suggested that the peak potential was related to the midpoint potential, the number of transferred electrons, and the rate of electron transfer between the electrode and protein−copper complex.

Plots for the voltammetric studies on β-syn and γ-syn are shown in Figure 4. β-syn demonstrated similar redox properties to that of α-syn, but γ-syn was strikingly different. The midpoint potentials for all three proteins were calculated using GPES manager and are listed in Table 3.

The midpoint potentials of α-syn and β-syn were similar but different from that of γ-syn. The peak current of oxidation and reduction was nearly identical for α-syn, which suggested that the redox cycling was fully reversible. However, the current response of reduction was less than the oxidation peak for γ-syn and β-syn. This indicated two possibilities: the oxidation was not reversible and part of the copper or protein might be oxidized permanently or the reduced copper(I) is lost due to the weak binding to protein. Two oxidation peaks were detected for γ-syn−Cu, suggesting the existence of two independent redox processes.

In order to investigate the observed effects in binding stability from the mutations on the redox activity of α-syn and β-syn, CV was employed on these mutants. Figure 5 compares wild-type α-syn with the mutants with either or both the histidine at position 50 and the N-terminus removed. For clarity, the data have had the background of apoprotein subtracted.

The voltammograms exhibited a second oxidation peak for the mutants α-syn △2−9 and H50A, which suggested that the coupled copper centers in these proteins might be split into two due to the mutation. However, the double mutant α-syn △2−9 H50A showed similar redox potential to that for WT α-syn. The midpoint potentials and integrated current peak charges are compared in Table 4.

Figure 6 compares the voltammograms for the C-terminal mutated or truncations. The oxidation and reduction peaks were significantly reduced on α-syn10−100 H50A and α-syn1−100, where the C-terminus was deleted. The redox peak for α-syn △119−126 was much higher compared to these two mutants. In addition, the redox potential was shifted when the 119−126 residues were knocked out, which suggested that this region was involved in copper coordination. The redox peak charges are compared in Table 5.

Figure 7 compares the voltammograms for β-syn and its N-terminal truncations and site-directed mutants. The redox activity of β-syn was enhanced when the His65 was substituted with alanine, while no increase was detected when residues 2−9 were knocked out although the peak potential was shifted. The ability of β-syn to exchange electrons in the electrode system was entirely annulled when the C-terminus was removed.

Only half of the copper centers on β-syn−Cu complex were redox reversible because the integrated reduction peak value was about 50% of oxidation charge. His65 might inhibit the redox activity especially the reduction of β-syn−Cu because the H65A β-syn mutant showed reversible electron cycling. The reduction peak was greatly diminished for β-syn △2−9, indicating amino acids 2−9 contributed to the reduction process. It was interesting that the oxidation intensity was regained for the double mutant β-syn △2−9 H65A, while the calculated reduction charge was not. This finding further confirmed that His65 inhibited the redox activity while the region 2−9 activated it. The lack of C-terminus on β-syn10−100 H65A led to complete abolition of redox activity, suggesting the C-terminus of the protein was critically involved in the electrochemistry.

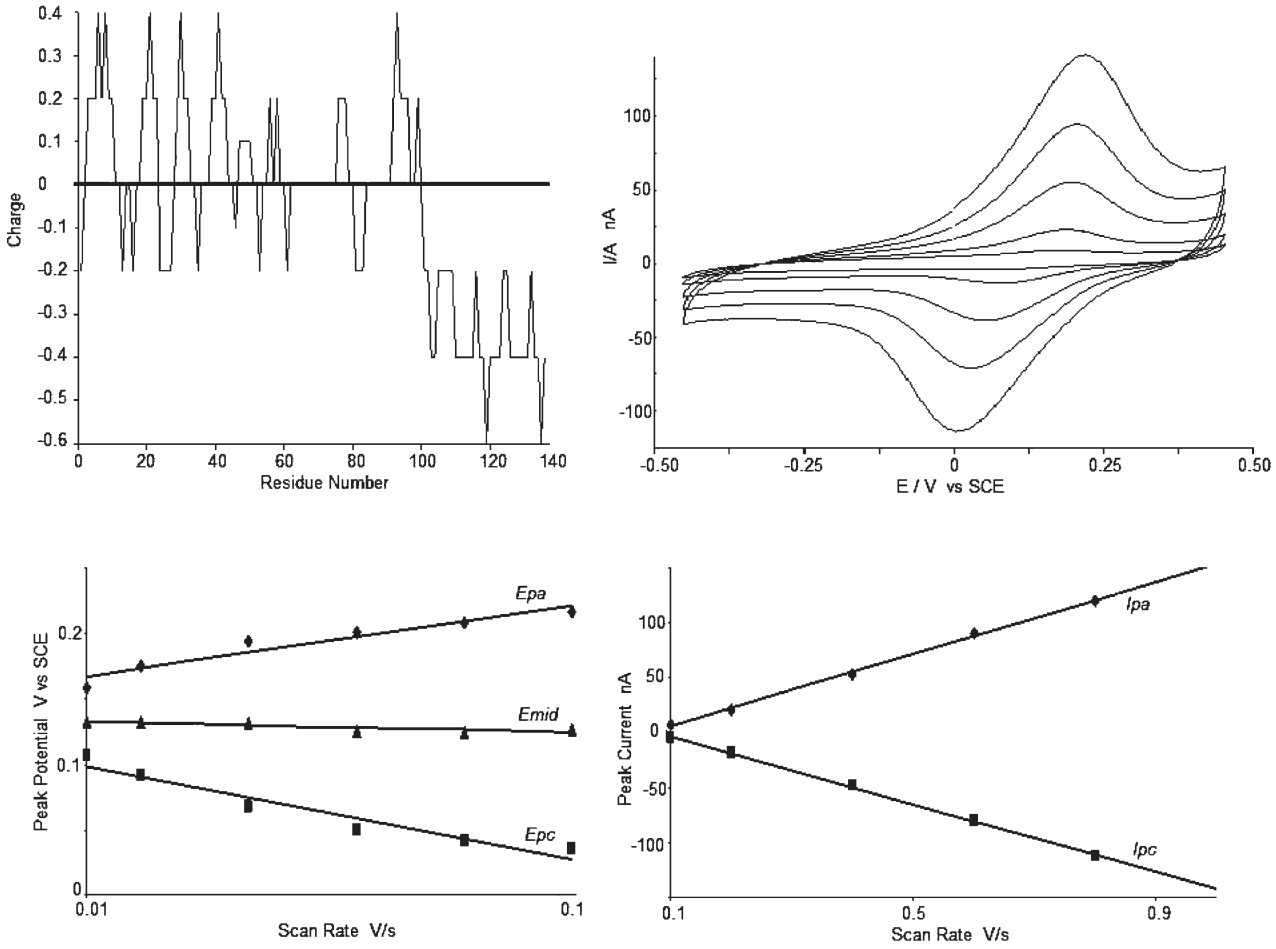

FIGURE 3: Voltammetric study of the copper centers on α-syn in 10 mM MOPS buffer at pH 7. (a, top left) The charge distribution across α-syn. (b, top right) Background subtracted voltammograms of copper-bound α-syn for scan rates from 10 to 80 mV s^{-1}. (c, bottom left) The logarithmic relationship between peak potential and scan rate. (d, bottom right) The linear relationship between peak current and scan rate.

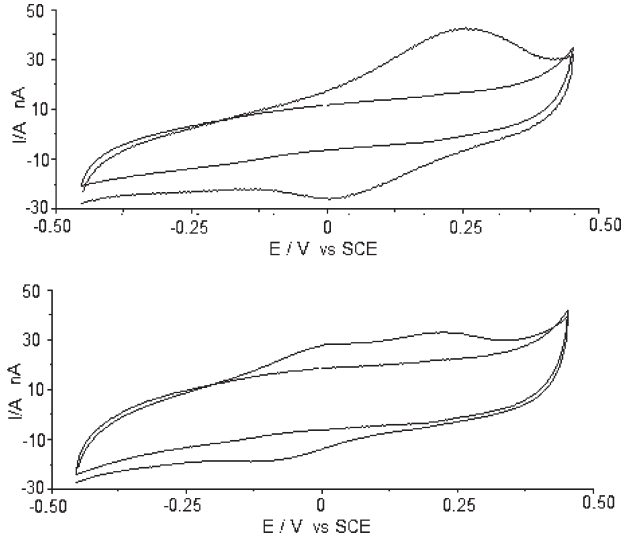

FIGURE 4: Cyclic voltammograms at a scan rate of 60 mV s^{-1} in 10 mM MES buffer, pH 7, for (a, top) copper-loaded β-syn and (b, bottom) copper-loaded γ-syn. The center trace on each voltammagram represents a background scan of apoprotein.

DISCUSSION

There has been an enormous amount of conflicting reports concerning the association of copper(II) to the synucleins, especially α-syn. Reports of the stoichiometric relationship of α-syn to copper(II) range from 1:1 (*35*) to 1:10 (*21*). Disassociation values range from 500 μM (*22*) to high nanomolar (*35*).

Table 3: Comparison of Midpoint Potentials for Copper-Loaded Synucleins[a]

	midpoint potential E_{mid} (V vs SCE)	
	first	second
α-syn	0.130 ± 0.003	not detected
β-syn	0.140 ± 0.007	not detected
γ-syn	−0.045 ± 0.005	0.065 ± 0.006

[a] $E_{mid} = {}^1/_2(E_{p,ox} + E_{p,red})$.

Isothermal titration calorimetry was used to assess the basic binding parameters of copper(II) to the synucleins. This technique is now very well established for the thermodynamic determination of small molecule−macromolecule interactions (*40*−*45*). It is also advantageous over many other methods as it looks at real-time binding events at concentrations significantly lower than necessary for EPR or NMR studies. Recently, a study was carried out by Hong et al. on the disease mutants associated with PD, using ITC and a chelated copper delivery system(*35*). In this study, the authors ruled out the possibility of ternary complex formation with glycine, copper, and the protein, making ITC highly suitable for this analysis. The purpose of this part of our study was to attempt to elucidate the contribution of various regions on the proteins to the coordination of copper(II). We can

report that copper(II) associates with all three synucleins in a 1:1 stoichiometry. This 1 to 1 relationship can be determined by the observation that, despite two distinct coordination modes existing, evident from the thermodynamic and EPR studies, the total stoichiometry from the addition of these two modes is around 1. This is most likely due to the synucleins being able to bind copper in either one or the other mode, so a solution of synuclein−copper(II) complexes will contain a mixture of proteins binding one atom of copper in either of the two coordination geometries. There is a clear preference for the higher affinity mode, hence an ~75% distribution bias in the two modes. There are slight deviations from 1:1 (no greater than 10%) evident from the thermodynamic data. This is likely due to the difficulty in accurately quantifying not only total protein but total protein available for copper chemistry. This was also a factor observed in the previous study (*35*).

The highest affinity for copper(II) is evident in γ-syn, with a disassociation constant in the picomolar range. To our knowledge, this is the first attempt to quantify the copper chemistry of γ-syn so no comparisons to previous work can be made. α-syn and β-syn bind copper(II) with a disassociation constant in the high nanomolar range, with α-syn displaying a slightly more stable complex. This finding for α-syn is in excellent agreement with a similar previous investigation (*35*), although this study only detected the two possible coordination modes in a disease-related mutant, A30P. A previous study on β-syn produced somewhat different findings, however, with two copper(II) sites present within the N-terminus in the submicromolar range (*46*). It is plausible that the circular dichroism method used by these researchers failed to accurately quantify the stoichiometry and may therefore have identified the two possible modes seen in our study. Other previous studies vary considerably for both the stoichiometry and affinity of copper(II) binding to α-syn. For example, one investigation reported that two coppers bound with micromolar affinity (*47*), but this study failed to account for the formation of insoluble copper hydroxide species that would be a factor if no chelator is used to deliver the metal. Other studies have reported from 2 (*22*) up to 10 molecules of copper bind with micromolar affinity (*21*). It is likely, however, that the use of glycine in this study prevented such low affinity associations, as the tight regulation of copper metabolism in vivo would also do.

The coordination of copper by α-syn has been studied in detail previously(*48*). While EPR analysis was only a small part of our investigation, the data suggest similar coordination by all three synuclein proteins. The two coordination modes apparent from the EPR data provide further confirmation of the two copper binding modes present on the synucleins. The cause of the distribution between species, with a 75% bias toward the mode with the highest affinity, is likely due to the preference for the metal to this mode. Of key interest, however, is the ability to track the effect on these coordination modes from the mutants by using

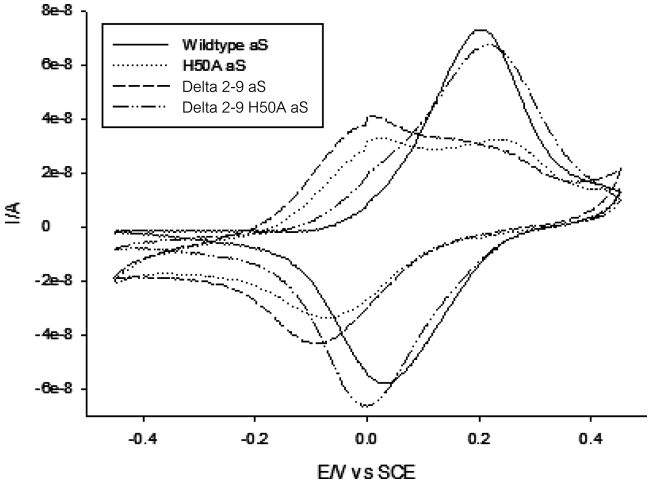

FIGURE 5: Comparison of voltammograms of site-directed and N-terminal truncated copper-loaded α-syn mutants with WT α-syn obtained at a scan rate of 60 mV s^{-1}. The experiments were conducted in 10 mM MES buffer, pH 7. The step potential was 0.0042 mV. aS = α-syn.

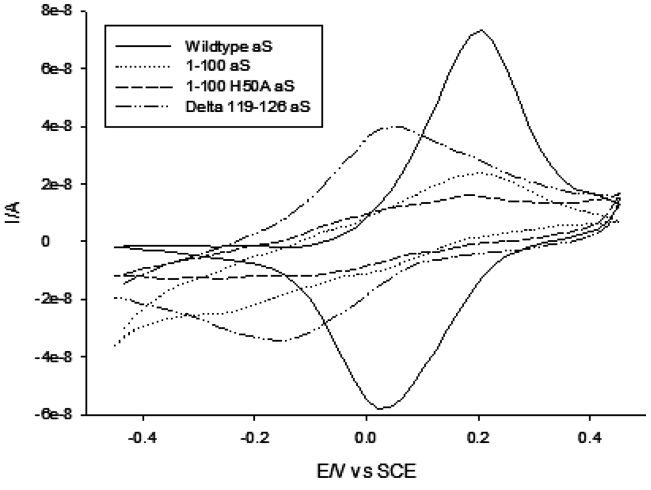

FIGURE 6: Comparison of voltammograms of site-directed and C-terminal truncated copper-loaded α-syn mutants with WT α-syn obtained at a scan rate of 60 mV s^{-1}. The experiments were conducted in 10 mM MES buffer, pH 7.

Table 4: Comparison of the Redox Data from Wild-Type α-syn and Various Mutants[a]

	midpoint potential E_{mid} (V vs SCE)			
	first	second	integrated oxidation peak charge (nC)	integrated reduction peak charge (nC)
α-syn	0.130 ± 0.003	not detected	3592 ± 222	−3638 ± 85
H50A	−0.030 ± 0.008	0.089 ± 0.006	2839 ± 140	−1167 ± 89
α-syn Δ2−9	−0.044 ± 0.007	0.077 ± 0.004	3788 ± 314	−2408 ± 71
α-syn Δ2−9 H50A	0.103 ± 0.002	not detected	4082 ± 91	−4195 ± 155
α-syn Δ119−126	−0.063 ± 0.005	not detected	2500 ± 318	−1241 ± 56
a-syn1−100	−0.024 ± 0.002	not detected	1007 ± 29	−236 ± 12
α-syn Δ2−9 H50A Δ119−126	0.092 ± 0.003	not detected	4775 ± 47	−2971 ± 24
α-syn10−100 H50A	0.032 ± 0.002	not detected	668 ± 12	−110 ± 3

[a] $E_{mid} = {}^1/_2(E_{p,ox} + E_{p,red})$.

Table 5: Comparison of the Redox Data from Wild-Type β-syn and Various Mutants[a]

	midpoint potential E_{mid} (V vs SCE)			
	first	second	integrated oxidation peak charge (nC)	integrated reduction peak charge (nC)
β-syn	0.140 ± 0.007	not detected	1719 ± 89	-931 ± 45
β-syn H65A	0.117 ± 0.002	not detected	2417 ± 74	-2389 ± 13
β-syn $\triangle$2−9	-0.083 ± 0.007	not detected	1208 ± 67	-307 ± 50
β-syn $\triangle$2−9 H65A	-0.055 ± 0.006	0.066 ± 0.002	3113 ± 106	-1178 ± 49

[a] $E_{mid} = {}^1/_2(E_{p,ox} + E_{p,red})$.

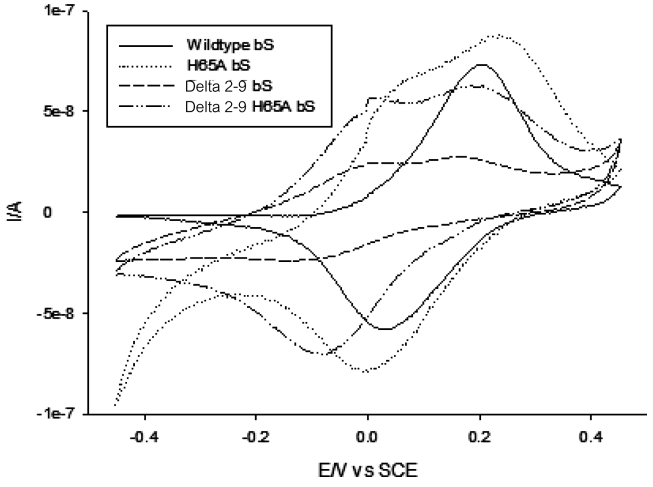

FIGURE 7: Comparison of voltammograms of site-directed and N-terminal truncated copper-loaded β-syn mutants with WT β-syn obtained at a scan rate of 60 mV s^{-1}. The experiments were conducted in 10 mM MES buffer, pH 7. bS = β-syn.

the enthalpy data from the wild-type proteins. The use of ITC in this study allows for the direct comparison of enthalpy values for individual sites between wild type and mutants. Although the reported enthalpies of binding in this study are very different from the ones reported by Hong et al., there are clear reasons for this. The total enthalpy recorded from the ITC consists of both the copper−glycine−protein reaction and the protonation chemistry of the buffer. In Hong's study, the buffer used was PIPES, which would contribute exothermically to the overall enthalpy change on the uptake of protons following copper binding to the protein (*49*). The MOPS buffer in this study, however, would have a significant endothermic effect on the overall enthalpy change during the reaction. The comparison of apparent enthalpy values is therefore valid as each experiment was carried out in identical conditions. It is clear from the thermodynamic data that the high affinity coordination mode observed in both α-syn and β-syn results primarily from the N-terminal region involving residues 2−9. When this region is removed, the high affinity binding mode with an enthalpy change of ~1.5 kcal/mol disappears. This region is therefore key to stable copper(II) coordination. The previously reported critical involvement of the histidine at position 50 in α-syn (*22*, *50*) is not supported by this study. In fact, from the data reported here, it would appear that both H50 in α-syn and H65 in β-syn reduce the stability of copper(II) binding when present. This lack of involvement for this histidine is supported by some more recent studies (*51*). Additionally, the previously suggested low affinity copper(II) site within the C-terminus (*24*) does not appear to bind copper independently but instead contributes to the coordination of the high affinity site within the N-terminus.

Of interest with any protein displaying high affinity for redox-active divalent cations is the issue of free radical chemistry. There is plenty of evidence for the role of oxidative stress in neurodegeneration, and the finding that a protein so closely associated with PD binds copper needs expanding upon. We have previously shown interesting redox properties for proteins involved in neurodegenerative disorders with stable copper(II) binding properties(*37*). The polar nature of the synucleins allows for the technique of electrostatically immobilizing proteins on electrodes and studying electron transfer kinetics to be used. From this study, all of the synucleins display interesting redox properties that are dependent on the copper(II) sites. α-syn is able to cycle electrons stably from its copper center and maintain the bound copper in both its copper(I) and copper(II) states. The implication is that the copper binding sites of the protein can bind either copper(I) and copper(II). The electrochemistry was completely dependent on the interaction with copper because no redox signal was detected on the apoprotein. The redox cycling was fully reversible, suggesting that the protein was unaffected by continuous oxidation and reduction of the copper ion. This is supported somewhat by a previous study demonstrating the potential of α-syn to maintain a stable Cu(I) coordination (*52*).

The electrochemical properties of α-syn were further examined by investigating the various mutants. The imidazole ring of His50 was believed to be involved in the copper coordination (*50*), and this study and others have clearly highlighted the importance of residues 2−9. Disruption of either of these regions has a significant effect on the midpoint potential of the copper center, with a negative shift of ~200 mV. The single mutations caused the split of the copper centers, and one of them lost the reductive feature, because two oxidation peaks were obtained on H50A α-syn and α-syn $\triangle$2−9 but the number of electrons transferred during the reduction process was about half of that during oxidation. This is consistent with the EPR and ITC data, which show a continued ability of the mutated protein to coordinate copper but with different enthalpy and stability values. The midpoint potential and responsive current peak during the redox process on the mutant α-syn $\triangle$2−9 H50A was quite close to that for WT α-syn, indicating the amino acids in the proximity might fill in the position and form the identical coordination geometry. There is evidence showing that lysine residues upstream of His50 could act as a copper anchoring site in the absence of histidine (*50*). Similarly, Asp2 might be substituted by Glu13, which could also provide nitrogen and oxygen ligand in the copper(II) binding mode (*22*). α-syn $\triangle$119−126 showed slightly decreased oxidative activity but large diminished reductive response. These observations suggest the redox capability of α-syn is dependent on copper and residues 2−9, His50, and the C-terminus. The integrated reduction peak charge was enormously reduced on α-syn1−100, indicating the presence of the C-terminal region of α-syn was essential for the reductive electrochemistry. The protein

might be oxidized permanently without the C-terminal region, which could lead to self-oligomerization and hence possible protein aggregation and neurodegeneration, supporting previous findings (*53*). It fits the hypothesis that C-terminal truncated α-syn constructs are more prone to fibrillate in vitro than the full-length protein (*54*−*56*). This is confirmed by a recent research revealing that the 125YEMPS129 motif in α-syn can modulate DA inhibition of α-syn fibrillization. However, α-syn ending before the 125YEMPS129 motif (residues 1−124) could still form soluble oligomers (*57*). In addition, the biochemically specific copper- or iron-mediated oxidative oligomerization turned out to be dependent upon the acidic C-terminus of α-syn because the C-terminally truncated proteins were not affected by both metals and hydrogen peroxide (*53*).

β-syn and *γ*-syn demonstrated significantly different redox properties, where the reduction peaks were of a lesser magnitude than the oxidation peaks. The findings indicate that some of the copper or protein might be oxidized permanently or copper(I) was not stable on the protein and was lost during the change in oxidation state. Interestingly, there were two independent redox centers on *γ*-syn, while only one was detected on α-syn or *β*-syn. These two sites on *γ*-syn suggest that in this case the two different binding modes for copper also result in sites where oxidation of the copper occurs differently.

In contrast to the H50A mutation of α-syn, mutation of His65 on *β*-syn enhanced the redox activity, especially the reduction current, producing reversible electron cycling. This demonstrated that His65 was responsible for the inhibition of the electrochemical activity of the protein. The reductive response was enormously diminished for *β*-syn △2−9 and *β*-syn10−100 H65A, indicating the involvement of residues 2−9 and the C-terminus on the redox activity.

These electrochemical findings for α-syn and *β*-syn provide a possible mechanism for the process of aggregation in PD and related disorders. There can be little doubt as to the involvement of both copper (*20*, *21*, *24*, *58*, *59*) and oxidative stress (*52*, *53*, *60*, *61*) on α-syn aggregation and fibrilization. This study, when looked at with other evidence for a protective role for the protein (*62*, *63*), must indicate the need to explore these redox properties further in terms of disease. There is, of course, also the possibility that these redox properties relate to the physiological function of the protein in either a neuroprotective or catalytic role.

We recently suggested that interactions between copper and α-syn can lead to the formation of a novel species of oligomers that are toxic when applied to cells exogenously or when induced in the cells(*20*, *64*). This would suggest that the copper−protein interaction is more likely to be associated with disease. In this case the redox activity of the protein may result in damage to cells. A recent paper by Wang et al. (*65*) provides support for this notion. This paper suggests that copper binding to the N-terminal region of α-syn could result in oxidative damage even before the protein forms aggregates. Their suggestion that α-syn binds copper in the form of Cu(I) is based on a limited CV study in solution in the presence of free copper. Their study only showed data for a single scan rate and did not report the relation between scan rate and neither peak potential nor peak current. Such analyses are necessary to ensure the measurements represent data from stable protein−metal complexes and not from unstable complexes that dissociate during the scan procedure. In contrast, our studies used all of these controls, multiple scan rates as well as removal of excess unbound copper from the protein. Therefore, the fully cycleable nature of the voltammograms for α-syn suggested by our study is more likely to be a true representation of the α-syn−metal complex redox activity. Despite these methodological concerns both this paper and our own work highlight the growing importance of α-syn−metal interactions in understanding the cellular role of α-syn in both health and disease.

REFERENCES

1. Burke, R. E. (2004) Recent advances in research on Parkinson disease: synuclein and parkin. *Neurologist 10*, 75–81.
2. Kotzbauer, P. T., Trojanowsk, J. Q., and Lee, V. M. (2001) Lewy body pathology in Alzheimer's disease. *J. Mol. Neurosci. 17*, 225–232.
3. Bodles, A. M., Guthrie, D. J., Harriott, P., Campbell, P., and Irvine, G. B. (2000) Toxicity of non-abeta component of Alzheimer's disease amyloid, and N-terminal fragments thereof, correlates to formation of beta-sheet structure and fibrils. *Eur. J. Biochem. 267*, 2186–2194.
4. Papadopoulos, D., Ewans, L., Pham-Dinh, D., Knott, J., and Reynolds, R. (2006) Upregulation of alpha-synuclein in neurons and glia in inflammatory demyelinating disease. *Mol. Cell. Neurosci. 31*, 597–612.
5. Adams, M. D., Kelley, J. M., Gocayne, J. D., Dubnick, M., Polymeropoulos, M. H., Xiao, H., Merril, C. R., Wu, A., Olde, B., and Moreno, R. F..; et al. (1991) Complementary DNA sequencing: expressed sequence tags and human genome project. *Science 252*, 1651–1656.
6. Kruger, R., Kuhn, W., Muller, T., Woitalla, D., Graeber, M., Kosel, S., Przuntek, H., Epplen, J. T., Schols, L., and Riess, O. (1998) Ala30Pro mutation in the gene encoding alpha-synuclein in Parkinson's disease. *Nat. Genet. 18*, 106–108.
7. Zarranz, J. J., Alegre, J., Gomez-Esteban, J. C., Lezcano, E., Ros, R., Ampuero, I., Vidal, L., Hoenicka, J., Rodriguez, O., Atares, B., Llorens, V., Gomez Tortosa, E., del Ser, T., Munoz, D. G., and de Yebenes, J. G. (2004) The new mutation, E46K, of alpha-synuclein causes Parkinson and Lewy body dementia. *Ann. Neurol. 55*, 164–173.
8. Singleton, A. B., Farrer, M., Johnson, J., Singleton, A., Hague, S., Kachergus, J., Hulihan, M., Peuralinna, T., Dutra, A., Nussbaum, R., Lincoln, S., Crawley, A., Hanson, M., Maraganore, D., Adler, C., Cookson, M. R., Muenter, M., Baptista, M., Miller, D., Blancato, J., Hardy, J., and Gwinn-Hardy, K. (2003) alpha-Synuclein locus triplication causes Parkinson's disease. *Science 302*, 841.
9. Golub, Y., Berg, D., Calne, D. B., Pfeiffer, R. F., Uitti, R. J., Stoessl, A. J., Wszolek, Z. K., Farrer, M. J., Mueller, J. C., Gasser, T., and Fuchs, J. (2009) Genetic factors influencing age at onset in LRRK2-linked Parkinson disease. *Parkinsonism Relat. Disord. 15*, 539–541.
10. Nishioka, K., Hayashi, S., Farrer, M. J., Singleton, A. B., Yoshino, H., Imai, H., Kitami, T., Sato, K., Kuroda, R., Tomiyama, H., Mizoguchi, K., Murata, M., Toda, T., Imoto, I., Inazawa, J., Mizuno, Y., and Hattori, N. (2006) Clinical heterogeneity of alpha-synuclein gene duplication in Parkinson's disease. *Ann. Neurol. 59*, 298–309.
11. Masliah, E., Rockenstein, E., Veinbergs, I., Mallory, M., Hashimoto, M., Takeda, A., Sagara, Y., Sisk, A., and Mucke, L. (2000) Dopaminergic loss and inclusion body formation in alpha-synuclein mice: implications for neurodegenerative disorders. *Science 287*, 1265–1269.
12. Hayashita-Kinoh, H., Yamada, M., Yokota, T., Mizuno, Y., and Mochizuki, H. (2006) Down-regulation of alpha-synuclein expression can rescue dopaminergic cells from cell death in the substantia nigra of Parkinson's disease rat model. *Biochem. Biophys. Res. Commun. 341*, 1088–1095.
13. Jakes, R., Spillantini, M. G., and Goedert, M. (1994) Identification of two distinct synucleins from human brain. *FEBS Lett. 345*, 27–32.
14. Davidson, W. S., Jonas, A., Clayton, D. F., and George, J. M. (1998) Stabilization of alpha-synuclein secondary structure upon binding to synthetic membranes. *J. Biol. Chem. 273*, 9443–9449.
15. Chandra, S., Chen, X., Rizo, J., Jahn, R., and Sudhof, T. C. (2003) A broken alpha-helix in folded alpha-synuclein. *J. Biol. Chem. 278*, 15313–15318.
16. Barnham, K. J., and Bush, A. I. (2008) Metals in Alzheimer's and Parkinson's diseases. *Curr. Opin. Chem. Biol. 12*, 222–228.
17. Lovell, M. A., Robertson, J. D., Teesdale, W. J., Campbell, J. L., and Markesbery, W. R. (1998) Copper, iron and zinc in Alzheimer's disease senile plaques. *J. Neurol. Sci. 158*, 47–52.
18. Pall, H. S., Williams, A. C., Blake, D. R., Lunec, J., Gutteridge, J. M., Hall, M., and Taylor, A. (1987) Raised cerebrospinal-fluid copper concentration in Parkinson's disease. *Lancet 2*, 238–241.

19. Gorell, J. M., Rybicki, B. A., Cole Johnson, C., and Peterson, E. L. (1999) Occupational metal exposures and the risk of Parkinson's disease. *Neuroepidemiology 18*, 303–308.
20. Wright, J. A., Wang, X., and Brown, D. R. (2009) Unique copper-induced oligomers mediate alpha-synuclein toxicity. *FASEB J. 23*, 2384–2393.
21. Paik, S. R., Shin, H. J., Lee, J. H., Chang, C. S., and Kim, J. (1999) Copper(II)-induced self-oligomerization of alpha-synuclein. *Biochem. J. 340* (Part 3), 821–828.
22. Rasia, R. M., Bertoncini, C. W., Marsh, D., Hoyer, W., Cherny, D., Zweckstetter, M., Griesinger, C., Jovin, T. M., and Fernandez, C. O. (2005) Structural characterization of copper(II) binding to alpha-synuclein: insights into the bioinorganic chemistry of Parkinson's disease. *Proc. Natl. Acad. Sci. U.S.A. 102*, 4294–4299.
23. Wolozin, B., and Golts, N. (2002) Iron and Parkinson's disease. *Neuroscientist 8*, 22–32.
24. Binolfi, A., Rasia, R. M., Bertoncini, C. W., Ceolin, M., Zweckstetter, M., Griesinger, C., Jovin, T. M., and Fernandez, C. O. (2006) Interaction of alpha-synuclein with divalent metal ions reveals key differences: a link between structure, binding specificity and fibrillation enhancement. *J. Am. Chem. Soc. 128*, 9893–9901.
25. Nielsen, M. S., Vorum, H., Lindersson, E., and Jensen, P. H. (2001) Ca^{2+} binding to alpha-synuclein regulates ligand binding and oligomerization. *J. Biol. Chem. 276*, 22680–22684.
26. Golts, N., Snyder, H., Frasier, M., Theisler, C., Choi, P., and Wolozin, B. (2002) Magnesium inhibits spontaneous and iron-induced aggregation of alpha-synuclein. *J. Biol. Chem. 277*, 16116–16123.
27. Uversky, V. N., Li, J., and Fink, A. L. (2001) Metal-triggered structural transformations, aggregation, and fibrillation of human alpha-synuclein. A possible molecular NK between Parkinson's disease and heavy metal exposure. *J. Biol. Chem. 276*, 44284–44296.
28. Sung, Y. H., Rospigliosi, C., and Eliezer, D. (2006) NMR mapping of copper binding sites in alpha-synuclein. *Biochim. Biophys. Acta 1764*, 5–12.
29. Kowalik-Jankowska, T., Rajewska, A., Wisniewska, K., Grzonka, Z., and Jezierska, J. (2005) Coordination abilities of N-terminal fragments of alpha-synuclein towards copper(II) ions: a combined potentiometric and spectroscopic study. *J. Inorg. Biochem. 99*, 2282–2291.
30. Rockenstein, E., Hansen, L. A., Mallory, M., Trojanowski, J. Q., Galasko, D., and Masliah, E. (2001) Altered expression of the synuclein family mRNA in Lewy body and Alzheimer's disease. *Brain Res. 914*, 48–56.
31. Buchman, V. L., Hunter, H. J., Pinon, L. G., Thompson, J., Privalova, E. M., Ninkina, N. N., and Davies, A. M. (1998) Persyn, a member of the synuclein family, has a distinct pattern of expression in the developing nervous system. *J. Neurosci. 18*, 9335–9341.
32. Ohtake, H., Limprasert, P., Fan, Y., Onodera, O., Kakita, A., Takahashi, H., Bonner, L. T., Tsuang, D. W., Murray, I. V., Lee, V. M., Trojanowski, J. Q., Ishikawa, A., Idezuka, J., Murata, M., Toda, T., Bird, T. D., Leverenz, J. B., Tsuji, S., and La Spada, A. R. (2004) Beta-synuclein gene alterations in dementia with Lewy bodies. *Neurology 63*, 805–811.
33. Daniels, M., and Brown, D. R. (2002) Purification and preparation of prion protein: synaptic superoxide dismutase. *Methods Enzymol. 349*, 258–267.
34. Hong, L., Bush, W. D., Hatcher, L. Q., and Simon, J. (2008) Determining thermodynamic parameters from isothermal calorimetric isotherms of the binding of macromolecules to metal cations originally chelated by a weak ligand. *J. Phys. Chem. B 112*, 604–611.
35. Hong, L., and Simon, J. D. (2009) Binding of Cu(II) to human alpha-synucleins: comparison of wild type and the point mutations associated with the familial Parkinson's disease. *J. Phys. Chem. B 113*, 9551–9561.
36. Brazier, M. W., Davies, P., Player, E., Marken, F., Viles, J. H., and Brown, D. R. (2008) Manganese binding to the prion protein. *J. Biol. Chem. 283*, 12831–12839.
37. Davies, P., Marken, F., and Brown, D. (2009) Thermodynamic and voltammetric characterization of the metal binding to the prion protein insights into pH dependence and redox chemistry. *Biochemistry 48*, 2610–2619.
38. Zhang, Y., Akilesh, S., and Wilcox, D. E. (2000) Isothermal titration calorimetry measurements of Ni(II) and Cu(II) binding to His, GlyGlyHis, HisGlyHis, and bovine serum albumin: a critical evaluation. *Inorg. Chem. 39*, 3057–3064.
39. Peisach, J., and Blumberg, W. E. (1974) Structural implications derived from the analysis of electron paramagnetic resonance spectra of natural and artificial copper proteins. *Arch. Biochem. Biophys. 165*, 691–708.
40. Ababou, A., and Ladbury, J. E. (2007) Survey of the year 2005: literature on applications of isothermal titration calorimetry. *J. Mol. Recognit. 20*, 4–14.
41. Ababou, A., and Ladbury, J. E. (2006) Survey of the year 2004: literature on applications of isothermal titration calorimetry. *J. Mol. Recognit. 19*, 79–89.
42. Bjelic, S., and Jelesarov, I. (2008) A survey of the year 2007 literature on applications of isothermal titration calorimetry. *J. Mol. Recognit. 21*, 289–312.
43. Cliff, M. J., Gutierrez, A., and Ladbury, J. E. (2004) A survey of the year 2003 literature on applications of isothermal titration calorimetry. *J. Mol. Recognit. 17*, 513–523.
44. Cliff, M. J., and Ladbury, J. E. (2003) A survey of the year 2002 literature on applications of isothermal titration calorimetry. *J. Mol. Recognit. 16*, 383–391.
45. Falconer, R. J., Penkova, A., Jelesarov, I., Collins, B. M. (2010) Survey of the year 2008: applications of isothermal titration calorimetry, *J. Mol. Recognit.* (in press).
46. Binolfi, A., Lamberto, G. R., Duran, R., Quintanar, L., Bertoncini, C. W., Souza, J. M., Cervenansky, C., Zweckstetter, M., Griesinger, C., and Fernandez, C. O. (2008) Site-specific interactions of Cu(II) with alpha and beta-synuclein: bridging the molecular gap between metal binding and aggregation. *J. Am. Chem. Soc. 130*, 11801–11812.
47. Bharathi, and Rao, K. S. (2007) Thermodynamics imprinting reveals differential binding of metals to alpha-synuclein: relevance to Parkinson's disease. *Biochem. Biophys. Res. Commun. 359*, 115–120.
48. Drew, S. C., Leong, S. L., Pham, C. L., Tew, D. J., Masters, C. L., Miles, L. A., Cappai, R., and Barnham, K. J. (2008) Cu^{2+} binding modes of recombinant alpha-synuclein—insights from EPR spectroscopy. *J. Am. Chem. Soc. 130*, 7766–7773.
49. Martell, A. E., and Smith, R. M. (1974) Critical stability constants, Plenum Press, New York and London.
50. Kowalik-Jankowska, T., Rajewska, A., Jankowska, E., and Grzonka, Z. (2006) Copper(II) binding by fragments of alpha-synuclein containing M1-D2- and -H50-residues; a combined potentiometric and spectroscopic study. *Dalton Trans.,* 5068–5076.
51. Lee, J. C., Gray, H. B., and Winkler, J. R. (2008) Copper(II) binding to alpha-synuclein, the Parkinson's protein. *J. Am. Chem. Soc. 130*, 6898–6899.
52. Lucas, H. R., Debeer, S., Hong, M. S., and Lee, J. C. (2010) Evidence for copper-dioxygen reactivity during alpha-synuclein fibril formation. *J. Am. Chem. Soc. 132*, 6636–6637.
53. Paik, S. R., Shin, H. J., and Lee, J. H. (2000) Metal-catalyzed oxidation of alpha-synuclein in the presence of copper(II) and hydrogen peroxide. *Arch. Biochem. Biophys. 378*, 269–277.
54. Crowther, R. A., Jakes, R., Spillantini, M. G., and Goedert, M. (1998) Synthetic filaments assembled from C-terminally truncated alpha-synuclein. *FEBS Lett. 436*, 309–312.
55. Serpell, L. C., Berriman, J., Jakes, R., Goedert, M., and Crowther, R. A. (2000) Fiber diffraction of synthetic alpha-synuclein filaments shows amyloid-like cross-beta conformation. *Proc. Natl. Acad. Sci. U. S.A. 97*, 4897–4902.
56. Murray, I. V., Giasson, B. I., Quinn, S. M., Koppaka, V., Axelsen, P. H., Ischiropoulos, H., Trojanowski, J. Q., and Lee, V. M. (2003) Role of alpha-synuclein carboxy-terminus on fibril formation in vitro. *Biochemistry 42*, 8530–8540.
57. Leong, S. L., Pham, C. L., Galatis, D., Fodero-Tavoletti, M. T., Perez, K., Hill, A. F., Masters, C. L., Ali, F. E., Barnham, K. J., and Cappai, R. (2009) Formation of dopamine-mediated alpha-synuclein-soluble oligomers requires methionine oxidation. *Free Radical Biol. Med. 46*, 1328–1337.
58. Bharathi, Indi, S. S., and Rao, K. S. (2007) Copper- and iron-induced differential fibril formation in alpha-synuclein: TEM study. *Neurosci. Lett. 424*, 78–82.
59. Capanni, C., Taddei, N., Gabrielli, S., Messori, L., Orioli, P., Chiti, F., Stefani, M., and Ramponi, G. (2004) Investigation of the effects of copper ions on protein aggregation using a model system. *Cell. Mol. Life Sci. 61*, 982–991.
60. Paik, S. R., Lee, D., Cho, H. J., Lee, E. N., and Chang, C. S. (2003) Oxidized glutathione stimulated the amyloid formation of alpha-synuclein. *FEBS Lett. 537*, 63–67.
61. Lucas, H. R., and Lee, J. C. (2010) Effect of dioxygen on copper(II) binding to alpha-synuclein. *J. Inorg. Biochem. 104*, 245–249.
62. Musgrove, R. E., King, A. E., and Dickson, T. C. (2010) Neuroprotective upregulation of endogenous alpha-synuclein precedes

ubiquitination in cultured dopaminergic neurons, *Neurotox. Res.* (in press).
63. Hashimoto, M., Hsu, L. J., Rockenstein, E., Takenouchi, T., Mallory, M., and Masliah, E. (2002) alpha-synuclein protects against oxidative stress via inactivation of the c-Jun N-terminal kinase stress-signaling pathway in neuronal cells. *J. Biol. Chem. 277*, 11465–11472.
64. Wang, X., Moualla, D., Wright, J. A., and Brown, D. R. (2010) Copper binding regulates intracellular alpha-synuclein localisation, aggregation and toxicity. *J. Neurochem. 113*, 704–714.
65. Wang, C., Liu, L., Zhang, L., Peng, Y., and Zhou, F. (2010) Redox reactions of the alpha-synuclein-Cu(2+) complex and their effects on neuronal cell viability. *Biochemistry 49*, 8134–8142.